A New Version of the Flusser Invariants Set for Pattern Feature Extraction

CONSTANTIN-IULIAN VIZITIU, DORU MUNTEANU
Communications and Electronic Systems Department
Military Technical Academy
George Cosbuc Avenue 81-83, Bucharest, Romania

Abstract: - The choice of an appropriate feature extraction method is essential for the success of the following recognition/classification process. This paper proposes a design method for a new pattern descriptors set belonging to the Flusser moments family, which is invariant to the elementary geometric transformations and respectively, has an increased noise robustness. Experimental results based on a real video image database, confirm the basic properties of this new descriptors set.

Key-Words: - Feature extraction, Flusser moments, pattern recognition, neural network

1 Introduction

In order to be useful in a pattern recognition process, the objects/patterns resulting after the input image segmentation must be represented in a suitable manner. This representation assumes some basic properties like: concision, redundant information discarding, invariance at elementary transforms and respectively, holds back of the information that is vital for pattern recognition success. This process known as *feature extraction*, is in a straight connection with the structure chosen for the input data representation, and is strongly dependent by the implemented application.

2 The Design Procedure for the Proposed Invariants Set

The design procedure for the proposed invariants set starts with the basic definition of the $(p+q)^{\text{th}}$-order complex moment for an integral function $f(x,y)$ [1], by the form:

$$c_{pq} = \int_{-\infty}^{\infty}\int_{-\infty}^{\infty} (x+\mathrm{i}y)^p (x-\mathrm{i}y)^q f(x,y)\mathrm{d}x\mathrm{d}y \quad (1).$$

It can be easily demonstrated that:

$$c_{pq} = \sum_{k=0}^{p}\sum_{s=0}^{q}\binom{p}{k}\binom{q}{s}(-1)^{q-s}\cdot \mathrm{i}^{p+q-k-s}\cdot m_{k+s,p+q-k-s} \quad (2),$$

where m_{pq} is the $(p+q)^{\text{th}}$-order geometrical moment.

The following important theorem [2] has been demonstrated:

"*If are performed the following conditions:* $n \geq 1$ *and* $\sum_{j=1}^{n} k_j\left(p_j - q_j\right) = 0,\ k_j, p_j, q_j \in \mathrm{Z}^+$, *then the product* $I = \prod_{j=1}^{n} c_{p_j q_j}^{k_j}$ *is invariant at rotation*".

The main disadvantage of the above descriptors set $\{I_k\}$ is produced by the fact that this is not invariant at all elementary geometrical transforms. An instant solution of this problem could be the following substitution $m_{pq} \to \eta_{pq}$ in equation (2):

$$c_{pq}^{(1)} = \sum_{k=0}^{p}\sum_{s=0}^{q}\binom{p}{k}\binom{q}{s}(-1)^{q-s}\cdot \mathrm{i}^{p+q-k-s}\cdot \eta_{k+s,p+q-k-s} \quad (3),$$

where η_{pq} is the $(p+q)^{\text{th}}$ -order centered geometrical moment.

Consequently, having as starting point this substitution, the translation and scaling invariance of η_{pq} moments [3], and applying the results of the Flusser theorem, it is relative easy to demonstrate that new descriptors set $\left\{I_k^{(1)}\right\}$ is invariant to the elementary geometrical transforms (in fact, to translation, scaling and rotation transforms). Generally speaking, this description modality generates complex values, and to obtain real values, it can hold back, for example, either its real part or its imaginary part.

To finalize the final form of the proposed invariants set, it is necessary to introduce a new type of $(p+q)^{\text{th}}$ -order complex moment [2], according to the following equation:

$$\lambda_{pq} = \int_{-\infty}^{\infty}\int_{\infty}^{\infty}(x-x_c+x_s)^p\,(y-y_c+y_s)^q\,\cdot \\ \cdot f(x,y)\,\mathrm{d}x\mathrm{d}y \quad (4),$$

where (x_c, y_c) are the coordinates of the input pattern centroid and the shift factors x_s and y_s are chosen accordingly [3]. Also, it can be demonstrated that the new central moments set can be normalized to ensure its invariance to translation and scaling by the following equation:

$$\xi_{pq} = \frac{\lambda_{pq}}{m_{00}^{\frac{p+q}{2}+1}} \quad (5).$$

In [4] has been demonstrated that, by introduction of the above shift factors, the most important advantage is the discarding of the standard central moments bugs in case of input symmetrical images use, simultaneously with the enhancement of the sensibility at noise action.

Obviously, because of a similar reason with one got by (3), it results an improved structure of the complex central moments, by the form:

$$c_{pq}^{(2)} = \sum_{k=0}^{p}\sum_{s=0}^{q}\binom{p}{k}\binom{q}{s}(-1)^{q-s}\cdot \\ \cdot \mathrm{i}^{p+q-k-s}\,\xi_{k+s,p+q-k-s} \quad (6).$$

Therefore, the final structure of the proposed invariants set can be rewritten by the form:

$$\begin{cases} \zeta_1 = c_{11}^{(2)} \\ \zeta_2 = c_{21}^{(2)}c_{12}^{(2)} \\ \zeta_3 = \mathrm{Re}\left(c_{20}^{(2)}c_{12}^{(2)^2}\right) \\ \zeta_4 = \mathrm{Im}\left(c_{20}^{(2)}c_{12}^{(2)^2}\right) \\ \zeta_5 = \mathrm{Re}\left(c_{30}^{(2)}c_{12}^{(2)^3}\right) \\ \zeta_6 = \mathrm{Im}\left(c_{30}^{(2)}c_{12}^{(2)^3}\right) \\ \zeta_7 = c_{22}^{(2)} \\ \zeta_8 = \mathrm{Re}\left(c_{31}^{(2)}c_{12}^{(2)^2}\right) \\ \zeta_9 = \mathrm{Im}\left(c_{31}^{(2)}c_{12}^{(2)^2}\right) \\ \zeta_{10} = \mathrm{Re}\left(c_{40}^{(2)}c_{12}^{(2)^4}\right) \\ \zeta_{11} = \mathrm{Im}\left(c_{40}^{(2)}c_{12}^{(2)^4}\right) \end{cases} \quad (7).$$

Consequently, the moments set proposed by the above equation has the following important properties:

– it is invariant at the elementary geometrical transforms (in fact, to rotation, translation and scaling operations);

– it eliminates the standard central moments bugs in case of symmetrical images;

– its robustness level to the noisy factors action inside of a classification system is more increased;

– it forms an independent base of pattern invariants (in sense of Flusser theorem [2]).

These theoretical properties of the proposed invariants set presented will be confirmed by the experimental results within next section.

3 Experimental Results

The input video database used for experimental part of this paper was made by three prototype-images (each representing an input class) of some modern aircrafts, as can be seen in fig. 1.

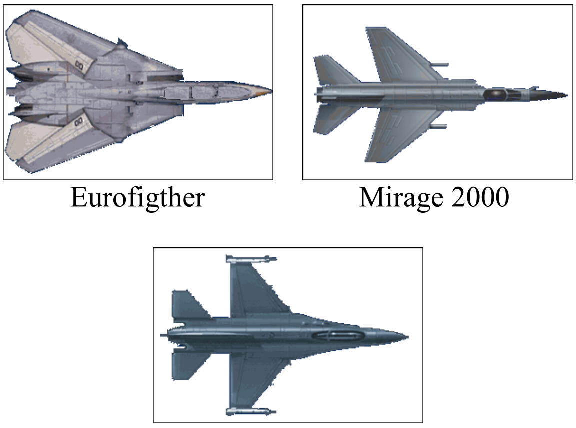

Fig.1: The prototype-images of video database used in experimental section (top view)

Each prototype-image has 128×128 resolution, in *.bmp* computing format.

To test the invariance property of the proposed invariants set at the elementary geometrical transforms, two prototype-images were translated, scaled and respectively, rotated in a proper manner [5]. In table 1, the results after the calculus of the moments set from (7) are indicated. Accordingly, it is relative easy to observe that invariance property of the proposed invariants set is accomplished.

To test the behavior of the proposed invariants set at the different kind of input image symmetries, a collection of standard images [4] has been used. In table 2, the results after moments calculus are indicated. Also, one can observe that the bugs of the standard central moments for symmetrical images (odd moments are zero) are eliminated.

The small differences that appear in case of the same order moments for different transforms applied to the input database are accountable by the digitization and processing errors caused by MATLAB software package.

Another interesting experimental problem is to make a comparative study between the invariants set got by (7) and the standard Flusser invariants set [2] having as reference point of view the influence of robustness level on the classification/recognition system performances. In fig. 2, the logical diagram for generating the input database used for classifier training/testing is presented. Also, supervised ART artificial neural network (SART) has been used as classifier.

Table 1

Moment	Transform	Reference images	Translation (pixels number)		Scaling (scaling factor)		Rotation (degree)	
			25	50	1.5	2	90°	180°
ζ_1	Eurofighter	-9.88e+003	-9.88e+003	-9.88e+003	-10e+003	-9.82e+003	-9,84e+003	-9,88e+003
	F16	-4.96e+003	-4.96e+003	-4.96e+003	-4.93e+003	-4.90e+003	-4,87e+003	-4,96e+003
ζ_2	Eurofighter	-8.62e+010	-8.62e+010	-8.62e+010	-8.76e+010	-8.52e+010	-8.57e+010	-8.58e+010
	F16	6.96+e005	6.96+e005	6.96+e005	6.92e+005	6.73e+005	6.83e+005	6.95e+005
ζ_3	Eurofighter	8.52e+014	8.52e+014	8.52e+014	8.65e+014	8.37e+014	8.47e+014	8.48e+014
	F16	2.94e+009	2.94e+009	2.94e+009	2.87e+009	2.78e+009	2.91e+009	3.12e+009
ζ_4	Eurofighter	-5.53e+006	-5.53e+006	-5.53e+006	-5.49e+006	-5.55e+006	-5.43e+006	-5.51e+006
	F16	**1.48e+007**	**1,48e+007**	**1,47e+007**	**1.43e+007**	**1.38e+007**	**1.41e+007**	**1.50e+007**
ζ_5	Eurofighter	7.43e+021	7.43e+021	7.43e+021	7.68e+021	7.27e+021	7.34e+021	7.36e+021
	F16	-1.17e+012	-1.17e+012	-1.17e+012	-1.21e+012	-0.95e+012	-1.23e+012	-1.20e+012
ζ_6	Eurofighter	3.21e+008	3.21e+008	3.22e+008	3.25e+008	3.34e+008	3.1e+008	3.25e+008
	F16	4.23e+009	4.23e+009	4.23e+009	4.27e+009	4.22e+009	4.31e+009	4.27e+009
ζ_7	Eurofighter	2.60e+008	2.61e+008	2.61e+008	2.66e+008	2.56e+008	2.52e+008	2.60e+008
	F16	6.39e+007	6.39e+007	6.39e+007	6.29e+007	6.22e+007	6.51e+007	6.42e+007
ζ_8	Eurofighter	-2.25e+019	-2.25e+019	-2.25e+019	-2.33e+019	-2.21e+019	-2.20e+019	-2.23e+019
	F16	-3.78e+013	-3.78e+013	-3.78e+013	-3.82e+013	-3.63e+013	-3.85e+013	-3.81e+013
ζ_9	Eurofighter	5.34e+011	5.34e+011	5.34e+011	5.39e+011	5.37e+011	5.27e+011	5.38e+011
	F16	-2.15e+008	-2.15e+008	-2.15e+008	2.10e+008	2.12e+008	2.20e+008	-2.17e+008
ζ_{10}	Eurofighter	1.94e+030	1.94e+030	1.94e+030	2.04e+030	1.92e+030	1.87e+030	1.92e+030
	F16	2.24e+019	2.24e+019	2.24e+019	2.32e+019	2.34e+019	2.27e+019	2.31e+019
ζ_{11}	Eurofighter	6.74e+002	6.74e+002	6.75e+002	6.81e+002	6.77e+002	6.83e+002	6.72e+002
	F16	3.21e+004	3.21e+004	3.21e+004	3.27e+004	3.25e+004	3.30e+004	3.23e+004

Experimental results obtained in case of invariance property testing

Table 2

Moment	The type of symmetry							
	Symmetry referred at both axes		**Symmetry referred at x axis**		**Symmetry referred at y axis**		**Symmetry referred at centroid**	
	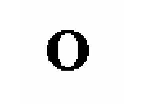	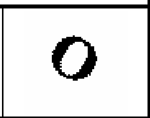	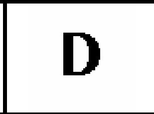	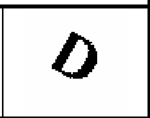	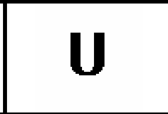	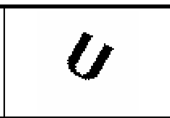	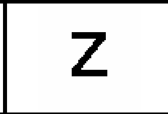	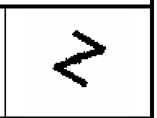
ζ_1	**0.36**	**0.38**	**0.31**	**0.33**	**0.32**	**0.35**	**0.45**	**0.45**
ζ_2	2.10e-006	1.97e-006	1.55e-005	1.62e-005	9.70e-005	10.2e-005	1.82e-005	1.93e-005
ζ_3	3.71e-008	3.82e-008	-1.34e-007	-1.21e-007	1.60e-006	1.47e-006	-3.69e-006	-3.71e-006
ζ_4	1.15e-007	0.98e-007	1.19e-007	1.14e-007	2.79e-004	2.70e-004	-1.91e-006	2.01e-006
ζ_5	3.88e-013	3.78e-013	-1.19e-009	-1.05e-009	-2.87e-008	-2.91e-008	7.62e-010	-7.65e-010
ζ_6	9.50e-013	9.43e-013	2.28e-009	2.24e-009	-7.62e-009	-7.58e-009	-9.48e-010	-9.43e-010
ζ_7	**0.14**	**0.16**	**0.11**	**0.138**	**0.132**	**0.152**	**0.27**	**0.27**
ζ_8	1.19e-008	1.23e-008	-1.76e-007	-1.81e-007	2.09e-006	2,19e-006	-1.92e-006	-1.86e-006
ζ_9	3.71e-008	3.67e-008	1.57e-007	1.61e-007	3.55e-007	3.58e-007	-1.38e-006	-1.42e-006
ζ_{10}	1.83e-014	1.81e-014	-1.10e-012	-0.98e-012	-4.91e-010	-4.97e-010	-2.97e-012	-2.95e-012
ζ_{11}	-1.31e-014	-1.27e-014	7.16e-012	7.27e-012	-1.73e-010	1.76e-010	-3.31e-011	-3.28e-011

Experimental results obtained in case of standard central moments bugs elimination

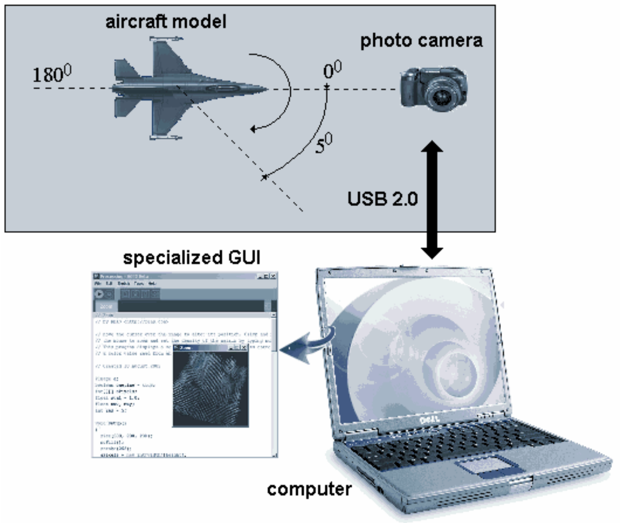

a) acquisition and preprocessing stage

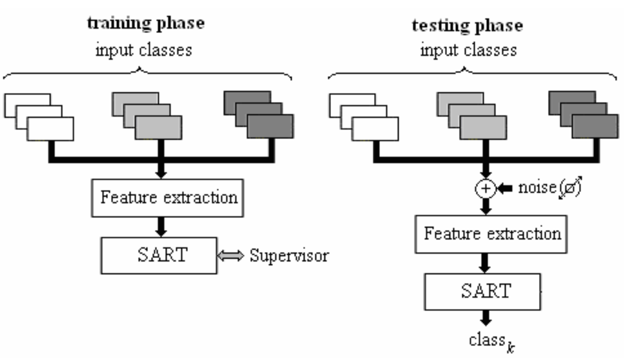

b) noise adding and classification stage

Fig.2: The testing procedure of robustness level

After the acquisition and preprocessing stage (see fig.2), a number of 37 video images/class resulted. For neural classifier training 19 images were used, while for testing 18 images were used, after noise adding. For testing of the classification system performances, each image was mixed with *salt and pepper* noise, and noise dispersion σ, as control parameter, has been modified in $[0, 0.1]$ range with a 10^{-2} increment.

After training and testing the SART classifier, it is interesting to analyze of the noise level influence (by moments calculus) on the classification performances. It has been computed the *good recognition score* (GRS) that represents in (%), the ratio between the number of correct classified input patterns and the total number of patterns used for classification).

Consequently, in fig.3, a graphic representation of the specific $\mathrm{GRS} = f(\sigma)$ dependence is indicated.

As it can be observed in fig.3, comparative with its standard version, a high level of the robustness to noise action for the proposed invariants set is demonstrated.

To demonstrate the property of the proposed invariants set to make an independent base (in sense of Flusser theory), on the video images database obtained after the acquisition and preprocessing stage, it will be applied a specific feature selection method (in fact, the Sammon projection algorithm, by $\mathrm{R}^{11} \to \mathrm{R}^n$ form). By help of this experiment, it will be followed if these eleven moments set contains an informational redundancy inside to him. Precisely, if preserving (or increased) the above classification performances, the dimension of the projection space can be decreased and then the proposed invariants set do not form an independent base for pattern description.

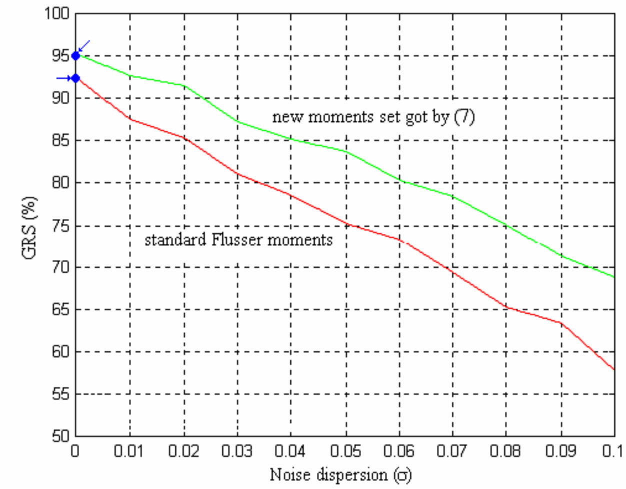

Fig.3: The graphic form of $\mathrm{GRS} = f(\sigma)$ dependence

In the next table, using the same classification diagram like one from the left side of fig. 2, the classification results are synthetically indicated.

Table 3

Feature selection	**Classification performances**
not ($n = 11$)	GRS: 95% SART training parameters: eradm= 10^{-2}; nepmax=10; nprmax=10 Training/testing time: 3.5 s
yes ($n = 10$)	GRS: 78% SART training parameters: eradm= 10^{-2}; nepmax=10; nprmax=10 Training/testing time: 3.1 s
yes ($n = 3$)	GRS: 52% SART training parameters: eradm= 10^{-2}; nepmax=10; nprmax=10 Training/testing time: 1.8 s

The classification results after Sammon projection algorithm applying

As it can be observed, trying to reduce the dimension of the feature space results in serious reducing of the GRS comparative with the case of feature selection method absence (see fig.4).

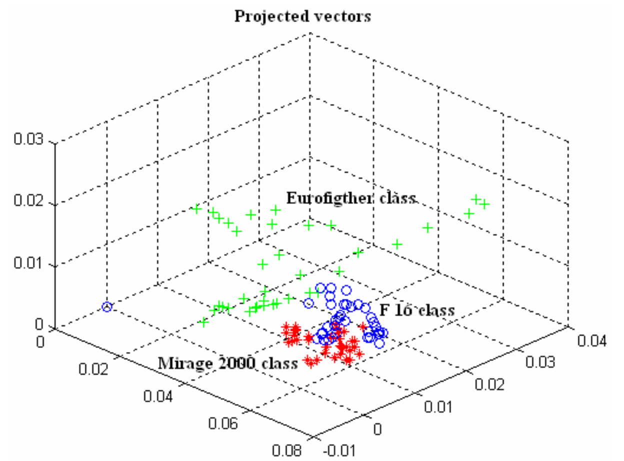

Fig.4: A 3D Sammon projection of the used database (accordingly with the last row from table 3)

More details regarding implementation aspects of the application presented in this section, in [5] and [6] are given.

4 Conclusions

The theoretical and experimental results reported in this paper allow the authors to formulate the following basic *remarks* concerning the proposed moments set properties:

– this moments set assures the invariance at the elementary geometrical transforms, eliminates the standard central moments bugs for symmetrical images, is more robust at the noise action than classic Flusser moments set and respectively, forms an independent base for pattern recognition;

– also, if this invariants set is used as feature description method inside of a real classification system, then the obtained GRS-s are very good and great in average, with 4% than standard Flusser moments (see fig.3).

It may be concluded that the *design procedure* of this new moments set as feature description algorithm within a classification system, *is feasible*.

References:

[1] A. Abo-Zaid, O. Hinton, and E. Horne, About moment normalization and complex moment descriptors, *Proceedings of ICPR*, 1988, pp. 399-407

[2] Flusser J., On the Independence of Rotation Moments Invariants, *Pattern Recognition Journal*, No.33, 2000, pp.1405-1410

[3] Ripley B.D., *Pattern Recognition and Neural Networks*, Cambridge University Press, 1966

[4] Rodrigues M., *Invariants for Pattern Recognition and Classification*, World Scientific Publishing Co., Danvers, 2000

[5] Vizitiu I.C., *Neural Networks used in Pattern Recognition*, MTA Publishing House, Bucharest, 2005

[6] Vizitiu I.C., A New Modality to Increase the Video Pattern Recognition Performances, *International Symposium on Defense Technology*, ZMNDU, Budapest, Hungary, 2006, pp. 416-443

Acknowledgments. The authors acknowledge the support of the Romanian Ministry of Education and Research through the Project AT 88 GR/2007 with the title "*An Inteligent System Design for Automatic Target Tracking and Recognition*".